Osteocyte-derived exosomes induced by mechanical strain promote human periodontal ligament stem cell proliferation and osteogenic differentiation via the miR-181b-5p/PTEN/AKT signaling pathway

Peiying Lv
Tianjin Medical University
Pengfei Gao
Affiliated Stomatilogy Hospital of Soochow University
Guangjie Tian
Tianjin Medical University
Yanyan Yang
Tianjin Medical University
Feifei Mo
Tianjin Medical University
Zihui Wang
Tianjin Medical University
Lu Sun
Harvard University of Dental Medicine
Mingjie Kuang
Provincial Hospital Affiliated to Shandong First Medical University
Yonglan Wang (tmuperiodontology@163.com)
Tianjin Medical University https://orcid.org/0000-0002-4149-6335

Research

Keywords: human periodontal ligament stem cells, mechanical strain, exosomes, miR-181b-5p, AKT signaling pathway

Posted Date: June 24th, 2020

DOI: https://doi.org/10.21203/rs.3.rs-21278/v2

Version of Record: A version of this preprint was published on July 17th, 2020. See the published version at https://doi.org/10.1186/s13287-020-01815-3.

Abstract

Background: The oral cavity is a complex environment in which periodontal tissue is constantly stimulated by external microorganisms and mechanical forces. Proper mechanical force helps maintain periodontal tissue homeostasis and improper inflammatory response can break the balance. Periodontal ligament (PDL) cells plays crucial roles in responding these challenges and maintaining the homeostasis of periodontal tissue. However, the mechanisms underlying PDL cell property changes induced by inflammatory and mechanical force microenvironments are still unclear. Recent studies have shown that exosomes function as a mean of cell-cell and cell-matrix communication in biological processes.

Methods: Human periodontal ligament stem cells (HPDLSCs) were tested by the CCK8 assay, EdU, alizarin red and ALP staining to evaluate the functions of exosomes induced by mechanical strain. MicroRNA sequencing was used to find the discrepancy miRNA in exosomes. In addition, RT-PCR, FISH, luciferase reporter assay and western blotting assay were used to investigated the mechanism of miR-181b-5p regulating proliferation and osteogenic differentiation through the PTEN/AKT pathway.

Results: In this study, the exosomes secreted by MLO-Y4 cells exposed to mechanical strain (Exosome-MS) contributed to human periodontal ligament stem cell (HPDLSC) proliferation and osteogenic differentiation. High-throughput miRNA sequencing showed that miR181b-5p was upregulated in Exosome-MS compared to the exosomes derived from MLO-Y4 cells lacking MS. The luciferase reporter assay demonstrated that miR-181b-5p may target Phosphatase tension homolog deletion (PTEN). In addition, PTEN was negatively regulated by overexpressing miR-181b-5p. PCR and western blot analyses verified that miR-181b-5p enhanced the protein kinase B (AKT) activity and improved downstream factor transcription. Furthermore, miR-181b-5p effectively ameliorated the inhibition of HPDLSC proliferation and osteogenesis induced by inflammation.

Conclusions: This study concluded that exosomes induced by mechanical strain promote HPDLSC proliferation and osteogenic differentiation via the miR-181b-5p/PTEN/AKT signaling pathway, suggesting a potential mechanism for maintaining periodontal homeostasis.

Introduction

The periodontium consists of the gingiva, periodontal ligament (PDL), root cementum and alveolar bone. The PDL plays a crucial role in periodontium homeostasis, repair, and nutrition [1, 2]. PDL fibers distribute the force to alveolar bone during the chewing movement, and PDL cells turn mechanical signals into biochemical signals that regulate various osteogenic-related pathways for periodontal tissue remodeling [3].

PDLSCs are adult stem cells and were first isolated from human PDL tissue [4]. These cells exhibit potential for self-renewal and multidirectional differentiation, which may be associated with mechanical loading from mastication or occlusion. PDLSCs subjected to static mechanical strain (SMS) show an increased proliferation rate and differentiation ability [5].

PDLSCs require a specific microenvironment to maintain their own undifferentiated and self-renewing state. This microenvironment is also known as the stem cell niche, and its activity depends on the interaction between cells[6]. Exosomes have been shown to function as a mean of intercellular communication in the body. Exosomes from PDLSCs promote bone regeneration and revascularization [7], and exosomes released in mechanical environments contribute to the maintenance of periodontal immune/inflammatory homeostasis [8]. Osteocytes are also mechanically sensitive cells and can secrete multiple biologically active factors to regulate bone remodeling. A previous study suggested that bone cells produce exosomes containing selective miRNAs that may be transferred to other organs [9].

Periodontitis is a bacteria-initiated inflammatory disease that causes periodontal soft and hard tissue loss and is the main cause of tooth loss in adults. The presence of a chronic inflammatory environment for a long duration changes the epigenetic characteristics of cells and reduces the regeneration capacity of periodontal tissue [5]. PDLSCs are important for the restoration of periodontal tissues as they are the main source of cells that form new attachments between periodontal tissues and root surfaces after periodontitis treatment [10-12]. Enhancing the regeneration capacity of HPDLSCs during an inflammatory challenge is one of the goals of treating periodontitis.

In this study, we present *in vitro* results demonstrating that exposure of MLO-Y4 cells to MS-derived exosomes could promote HPDLSC proliferation in an inflammatory environment. Moreover, we show that miR-181b-5p-mediated activation of the PTEN/PI3K/AKT axis is the key factor for this effect.

Materials And Methods

Cell culture

Human PDLSCs were isolated from extracted premolars and impacted third molars where obtained from systemically healthy adults for orthodontic purpose (18-25 years of age) with written informed consent and, and was under approved guidelines set by the Ethics Committee of Tianjin Medical University Stomatological Hospital. Primary cells were cultured as previously reported [13]. All HPDLSCs used in this study were at passage 3-5.

Murine osteocyte-like (MLO-Y4) cells were cultured in α-MEM containing 5% fetal bovine serum and 5% calf serum with penicillin-strepomycin in flasks precoated with rat tail collagen type I.

Colony-forming unit (CFU) assay

HPDLSCs (P4, 1×10^3 cells/plate) were seeded onto 100mm culture dishes and cultured for 12days. Next, the cells were fixed by 4% formaldehyde and then stained with 0.1% crystal violet (Sigma).

Osteogenic differentiation assay

HPDLSCs (2×10^5 cells/well) were cultured in 6-well plates containing osteogenic differentiation medium (Cyagen, Suzhou, China). The medium was refreshed every 3 days until the 21st day. Cells were fixed with

4% paraformaldehyde. Mineralized nodules were observed by staining with the 1% Alizarin red solution (Cyagen, Suzhou, China). The activity of alkaline phosphatase (ALP) was analyzed using an Alkaline Phosphatase Staining Kit (MKbio, Shanghai, China). Staining images were acquired using an inverted microscope, and ImageJ was used to analyze the images.

Adipogenic differentiation assay

HPDLSCs (2×10^5 cells/well) were cultured in 6-well plates containing adipogenic differentiation medium (Cyagen, Suzhou, China) for 21 days. Next, cells were fixed with 4% paraformaldehyde. Oil droplets were observed by staining with the Oil Red O solution (Cyagen, Suzhou, China).

Flow cytometric analysis

HPDLSC surface markers were analyzed by flow cytometry. HPDLSCs (P4) were trypsinized and adjusted to 5×10^6 cells/mL, and 1 μg of antibody (CD45, CD146, CD90 and CD73; eBioscience, San Jose, CA, USA) was added to 200 μl of cell suspension. The samples were incubated at 4°C in the dark for 2 h and centrifuged at 800 r/min for 5 min. The supernatant was discarded, and the cell pellet was washed twice with PBS and resuspended in 200 μl of PBS for flow cytometry analysis (Beckman Coulter, CA, USA).

Mechanical strain loading on MLO-Y4 cells

FBS was centrifuged at 4000×g for 15 min and then at 100,000×g for 70 min to sediment and concentrate EVs followed by filtration through a 0.22 μm filter membrane for exosome-depleted FBS preparation. Cells were exposed to mechanical strain (MS) by the Flexcell Tension Plus system (FX-4000T, Flexcell International, Burlington, NC). MLO-Y4 cells were seeded into 6-well Bioflex plates (Flexcell International, Burlington, NC) at a density of 1×10^5 cells/well and incubated for 24 h. The cells were then replaced with culture medium containing 10% exosome-depleted FBS. The experimental group was subjected to cyclic stretch with 8% shape variable at a frequency of 0.1 Hz for 30 min and the cell culture supernatant was collected after 24 h. The same operation was performed again in the next 3 days. The supernatant from the control groups was collected every 24 h for 3 days.

Exosomes isolation, purification and identification from MLO-Y4 cell culture supernatants

Briefly, cell culture supernatants were centrifuged at 300×g for 15 min to remove cells, filtered through a 0.22 μm filter membrane to remove cellular debris, and ultracentrifuged at 100,000×g for 70 min. The isolated pure exosomes were collected and stored at −80°C for future use.

Nanoparticle tracking analysis (NTA), transmission electron microscopy (TEM), and western blotting assay were used to identify the collected particles. Absolute size distribution of exosomes was directly tracked by the NanoSight NS 300 system (NanoSight Technology, Malvern, UK). The collected exosomes were adjusted to 10^6/ml. Under 450 nm laser irradiation, the camera recorded for 1 min at 25 frames/second, and this process was repeated 3 times. According to the Brownian motion of exosomes,

the Einstein equation was used to calculate the concentration and hydrodynamic diameter of the exosomes.

The morphology and diameter of exosomes were investigated using TEM (Hitachi HT7700 TEM, Tokyo, Japan). The exosome sample (10 μl) was placed on a copper net with a pore size of 2 nm followed by incubation at room temperature for 2 min. Filter paper was used to drain the liquid from the side of the filter. The sample was then negatively stained with 2% phosphotungstic acid solution (pH 7.0) for 1 min and then submitted to TEM for observations.

In addition, the exosomal surface-specific proteins CD63, CD81 and Alix were detected by western blotting assay.

Cell viability and proliferation assay

Cell proliferation was measured using the Cell Counting Kit-8 (Dojindo, Japan) according to the manufacturer instruction. HPDLSCs were cultured in a 96-well plate (2×10^4 cells/well) and subjected to the following treatments: PBS, *Porphyromonasgingivalis* lipopolysaccharide (Pg.LPS) (San Diego, CA, USA) (1 μg/mL), LPS + exosomes from normally cultured cells (Exosome); exosomes from MS-treated cells (Exosome-MS), and combination of LPS+Exo-MS. The OD value was recorded from day 0 to day 4 of culture. The absorbance was measured using a microplate reader (Bio-Tek, USA) at a wavelength of 450 nm.

5-Ethynyl-2'-deoxyuridine (EdU) staining

DNA replication activity was evaluated by EdU apollo 567 in vitro kit (Solarbio, Beijing, China) to further confirm the HPDLSC proliferation rate according to the manufacturer's instructions. HPDLSCs were plated into a glass-bottom plate at a density of 1×10^5 cells and treated by working solution for 24 h. Cell culture medium of all groups was replaced with the mixture and incubated at 37°C for 2 h. After incubation, cells were fixed with 4% paraformaldehyde at 4°C for 30 min and then washed three times with PBS. Cells were permeabilized with 0.1% Triton X-100 for 2 min on ice and washed twice with PBS. Nuclei were stained with DAPI (Sigma, USA). Images were captured with a confocal fluorescence microscope.

High-throughput miRNA sequencing

The high-throughput sequencing service and subsequent bioinformatics analysis were provided by BGI Biotech (Shenzhen, China). Briefly, miRNA was purified from exosome total RNA using the TaqMan ABC miRNA Purification Kit (Thermo Scientific, USA) following the manufacturer's instructions. RNA libraries were generated and sequencing was performed using BGISEQ-500. The differential expressed miRNA was identified by BGI with the value of log2-Ratio>1 and Q value<0.001. Gene ontology and KEGG pathway analyses were based on NCBI.

miRNA fluorescence in situ hybridization (FISH)

The subcellular localization of miRNA was determined by FISH, which was conducted as previously reported [14]. The FAM-5’-CCCACCGACAGCAATGAATGT-3’ probe was synthesized from the sequence of miR-181b-5p. In situ hybridization was conducted according to the instructions of the FISH Detection Kit (QIAGEN, Germany) followed by counterstain with DAPI. Images were acquired with a confocal fluorescence microscope.

Transient transfection

HPDLSCs were seeded into 6-well plates (5×10^5 per well) and incubated for 24 h. Cells were either left untreated or transiently transfected with miR-181b-5p mimics, mimics NC, inhibitors and inhibitors NC (Ribobio, Guangzhou, China) using Lipofectamine 2000 (Invitrogen, USA) according to the manufacturer’s instructions. Briefly, miR-181b-5p mimics (50 nM), mimics NC (50 nM), inhibitors (100 nM), and inhibitors NC (100 nM) were separately mixed with diluted Lipofectamine 2000 at room temperature for 20 min. The mixtures were then cultured with cells for 48 h. The following sequences were used: miR-181b-5p mimics NC sense 5’-UUC UCC GAA CGU GUC ACG UTT-3’ and antisense 5’-ACG UGA CAC GUU CGG AGA ATT-3” miR-181b-5p inhibitor 5’-ACCCACCGACAGCAAUGAAUGUU-3’; and miR-181b-5p inhibitor NC 5’-CAG UAC UUU UGU GUA GUA CAA-3’.

Luciferase reporter assay

TargetScan, microT, PITA and miRanda were used to predict the potential miR-181b-5p-binding site in the 3' untranslated region (3'-UTR) of the wild and mutant PTEN gene. HPDLSCs were seeded into 24-well plates (1×10^5 per well) for the luciferase reporter assays, and cells in each well were cotransfected with a pmir-GLO Dual-Luciferase miRNA Target Expression Vector (containing a wild-type or mutant PTEN 3'UTR; Promega, USA) and miR-181b-5p mimics, mimics-NC, inhibitor or inhibitor-NC using the Attractene Transfection Reagent Kit (Invitrogen, USA). The luciferase activity was assayed using a Dual Luciferase Reporter Assay Kit (Promega, USA) 24 h posttransfection according to the manufacturer's instructions.

Biotin-coupled miRNA capture

Because PTEN plays an important role in regulating cell proliferation and is one of the miR-181b-5p target genes, a pull-down assay was performed to investigate whether miR-181b-5p directly binds to PTEN. Briefly, HPDLSCs were transfected with biotinylated miRNA mimics or nonsense control (NC) (GenePharma, Shanghai, China), and cells were collected at 48 h after transfection. The biotin-conjugated RNA complex was pulled down using streptavidin-coated magnetic beads (Pierce Biotechnology, USA). The bound mRNA was purified using a RNeasy Mini Kit (QIAGEN, Germany). The enrichment of PTEN mRNA was evaluated by real time-PCR analysis.

Western blotting assay and antibodies

Cells were lysed using RIPA buffer to obtain total protein, and exosomal protein was extracted using a ProteoPrep® Total Extraction Sample Kit (Sigma-Aldrich, USA) following the manufacturer’s protocol.

Protein concentration was measured using a BCA Protein Assay Kit (Thermo Fisher Scientific, USA). Equivalent amounts of proteins were then electrophoresed on SDS-PAGE and transferred onto PVDF membranes. Membranes were blocked using 5% BCA for 2 h at room temperature and incubated with primary antibodies at 4°C overnight. After three PBST washes, membranes were incubated with secondary antibodies at 37°C for 1 h. ECL solution was then prepared, and the bands on the membranes were scanned and imaged in a dark room. The results were quantified using ImageJ. GAPDH was used as an internal control.

Real time-PCR

Total RNA was extracted from the cells using TRIzol reagent (Invitrogen, USA). The concentration and purity of the RNA were measured using a NanoDrop One Microvolume UV-Vis Spectrophotometer (Thermo Fisher Scientific, USA) according to the manufacturer's instruction. The Prime Script RT Reagent Kit (TaKaRa, Japan) was used for reverse transcription according to the manufacturer's instructions. The SYBR Premix Ex Taq II Kit (TaKaRa, Japan) was used for real time-PCR analysis using the Roche Light Cycler 480 sequence detection system (Roche Diagnostics, Switzerland). GAPDH or U6+miR16 was used as an internal control.

Statistical analysis

All data were presented as the means ± standard deviation (SD). The data of each group were tested for homogeneity, and the results were analyzed by one-way analysis of variance and minimum significant difference test (Fisher’s least significant difference [LSD]). $P<0.05$ was considered as statistically significant, $P<0.01$ and $P<0.001$ were considered as highly significant. All statistical analyses were performed using SPSS 23.0 (IBM Corp., USA).

Results

Characterization of HPDLSCs

HPDLSCs exhibited typical long spindle-shaped morphology and were arranged in a vortex observed by inverted microscope (Sup. Fig.1A). CFU-F assay confirmed that HPDLSCs were able to form cell clusters (Sup. Fig.1B). For osteogenic and adipogenic differentiation assay, mineralized nodules and lipid droplets were detected after induction(Sup. Fig.1C-D). Flow cytometry analyses showed that these cells were highly positive for the mesenchymal stem cell-positive markers CD73, CD146 and CD90, but were negative for CD45 (Sup. Fig.1E). These findings indicated that HPDLSCs had basic characteristics of mesenchymal stem cells.

Characterization of exosomes derived from MLO-Y4 culture supernatants

NTA, TEM, and western blotting assay were used to identify the purified exosomes. TEM showed that MLO-Y4-Exos exhibited a round morphology with a size ranging from 30 to 100 nm (Fig. 1A). Western blotting assay showed that MLO-Y4-Exos were positive for the characteristic exosomal surface markers

including CD63, CD81 and Alix (Fig. 1B). The NTA measurements revealed that the size of these particles varied from 30 to 100 nm (Fig. 1C). The exosome particle size distribution intensity is shown in Fig. 1D. Therefore, these analyses confirmed that the MLO-Y4-derived particles collected in our experiments are exosomes.

Effects of Exosome-MS on the proliferation of HPDLSCs

To investigate the functional roles of exosomes derived from MLO-Y4 cells subjected to mechanical strain (Exosome-MS) on cell proliferation under normal or inflammatory conditions, HPDLSCs were treated with Pg.LPS or normal media for 12 h followed by coculture with Exosome or Exosome-MS treatments for a series of functional assays. From day 2, the CCK-8 results revealed that the cell proliferation rate in the Exosome-MS group increased compared to that in the control group ($P<0.05$) and that the LPS treatment markedly reduced the proliferative capability of cells ($P<0.05$) (Fig. 2B). In addition, the LPS-induced downregulation of proliferation was rescued by Exosome-MS, whereas Exosome did not significantly differ from the control group. To confirm the ability of Exosome-MS to promote proliferation, an EdU assay was performed (Fig. 2C). The EdU assay result was the similar as that of the CCK-8 assay (Fig. 2D). These results indicated that exosomes produced by mechanically stimulated cells promote proliferation, even in an inflammatory environment, and reduce the inhibitory effects of inflammation but that exosomes produced from unstimulated cells do not have these effects.

Effects of Exosome-MS on osteogenic differentiation of HPDLSCs

HPDLSCs were cultured in osteogenic differentiation medium, and Alizarin red staining was used to evaluate the calcium nodule-forming ability. The ALP staining results showed that the staining areas in the Exosome-MS group were significantly larger than that in the control group, and the staining in the Exosome-MS group was also more intense than that in the control group (Fig.3A). There were less staining areas in the LPS and LPS+Exosome groups, and the staining areas in these groups were significantly different from that in the LPS+Exosome-MS group. The Alizarin red staining results were the similar as the ALP staining results (Fig.3B). The expression of BMP2 and Runx2 was upregulated in Exosome-MS group. Among the three groups of cells treated with LPS, the gene expression level of the LPS+Exosome-MS group was higher than that in the LPS group. However, there was no significant statistical difference between the LPS+Exosome group and the LPS group (Fig.3E-3F). Thus, these findings suggested that Exosome-MS not only promotes proliferation but also promotes osteogenic differentiation of HPDLSCs even in an inflammatory environment.

Analysis of functional attributes connected to Exosome-MS changes in gene sets and signaling pathways

We explored the molecular biological mechanisms of Exosome-MS in promoting cell proliferation and osteogenic differentiation. miRNA-seq was performed to detect differential gene expression between Exosome-MS and Exosome. A total of 121 targets were upregulated and 85 targets were downregulated in Exosome-MS compared with Exosome, and the results were illustrated using a heat map (Fig. 4A and

4B). GO enrichment analysis suggested that the miRNAs in Exosome-MS play a key role in metabolic processes (Fig. 4C and 4D). KEGG pathway enrichment analysis was performed to evaluate the characteristics of exosome-mediated gene expression (Fig. 4E). Related genes were more abundant in environmental signal transduction and infectious diseases.

miR-181b-5p targets to PTEN

Among the differentially expressed microRNAs, miR-181b-5p was selected for further research (Sup.Fig.3). Recent studies have shown that miR-181b-5p plays an important role in regulating cell proliferation, apoptosis [15] and the immune inflammatory response [16]. miR-181b-5p expression was upregulated in Exosome-MS (Fig. 5A). FISH assays showed that miR-181b-5p was mainly located in the cytoplasm of HPDLSCs treated with exosomes and that the Exosome-MS group had a higher fluorescence intensity than the Exosome group (Fig. 5B).

We screened the PITA (http://genie.weizmann.ac.il) [17], DIANA microT (http://diana.imis.athena-innovation.gr/DianaTools/index.php?r=microT_CDS/index) [18], TargetScan (http://www.targetscan.org) [19] and miRnada (http://www.microrna.org) [20] databases to predict the target genes of miR-181b-5p. We obtained 157 crossover genes. Phosphatase tensin homolog deletion (PTEN) is closely related to cell growth and apoptosis [21]. The results showed that miR-181b-5p is predicted to interact with wild-type and mutant PTEN (Fig. 5D), and the luciferase assay also revealed that miR-181b-5p interacted with PTEN (Fig. 5G). real time-PCR showed that overexpression of miR-181b-5p inhibited PTEN expression (Fig. 5E) and that suppression of miR-181b-5p upregulated PTEN expression (Fig. 5F). To detect whether miR-181b-5p directly binds to PTEN, miR-181b-5p was labeled with biotin, and the enrichment observed in the Biotin-miR-181b-5p group was 4.7-fold greater than that in the control group (Fig. 5H).

Exosomal miR-181b-5p regulates HPDLSC proliferation through the PTEN/AKT signaling pathway

The PI3K/Akt signaling pathway is one of the most important pathways for cell survival, cell growth, glucose metabolism and protein synthesis in host cells [22], and PTEN negatively regulates the PI3K/Akt pathway. To verify the mechanisms of exosomal miR-181b-5p promoting HPDLSC proliferation, real time-PCR was performed to investigate the related genes including PTEN, cyclin D1 (CCDN1), phosphoinositide-3-kinase regulatory subunit 1 (PI3KR1), phosphatidylinositol-4,5-bisphosphate 3-kinase catalytic subunit alpha (PI3KCA) in the PTEN/PI3K/Akt signaling pathway. The results showed that CCDN1, PI3KR1, and PIK3CA were upregulated in the miR181b-5p mimics group but downregulated in the miR181b-5p inhibitor group (Fig.6A-6C). PTEN showed the opposite trend (Fig.6D). In addition, western blotting assay was performed to further verify the AKT phosphorylation level (Fig.6E-6G). In the miR181b-5p mimics group, PTEN expression was down-regulated, while pAKT expression was up-regulated. miR181b-5p inhibitor group showed the opposite trend. In addition, after adding PTEN inhibitor BPV(PHEN) (Biovision, USA), pAKT expression was significantly upregulated in the miR181b-5p mimic group, while pAKT expression was downregulated in the miR181b-5p inhibitor group compared to the control group (Fig.6H-6I). The results showed that miR181b-5p inhibited PTEN, thereby phosphorylating AKT and regulating its downstream factors.

Exosomal-MS regulates HPDLSC osteogenic differentiation via miR-181b-5p

To verify the mechanisms of Exosome-MS in promoting HPDLSC osteogenic differentiation under inflammatory conditions, real time-PCR was performed to investigate related genes including bone morphogenetic protein-2 (BMP2) and RUNX family transcription factor 2 (Runx2). In addition, ALP and Alizarin red staining assays were performed after 21 days of induction (Fig.7A-7C). The results showed that addition of miR-181b-5p mimics to the LPS+Exosome group changed LPS inhibition of BMP2, Runx2, AKT1 and PI3KCA expression, but the miR-181b-5p inhibitor downregulated gene expression in the LPS+Exosome-MS group (Fig.7D-7G). These results demonstrated that Exosome-MS regulates osteogenic differentiation through miR-181b-5p.

Discussion

Mechanical stimulation plays an essential role in regulating bone remodeling and maintaining bone homeostasis [23], and PDLSCs are indispensable in this process [24]. Therefore, exploring the cell niche changes of PDLSCs in a mechanical environment is beneficial to further understand the role of occlusal force in the reconstruction of periodontal tissues. In our study, MLO-Y4-Exos induced by MS promoted proliferation and osteogenic differentiation of HPDLSCs and rescued the inhibitory effects of LPS-induced inflammation, which were mediated by the miR-181b-5p/PTEN/AKT axis.

Previous studies have focused on the regulation of osteogenesis by periodontal ligament cells under mechanical force. It was reported that PDLSCs maintain bone homeostasis during tooth movement by regulating the balance between osteoblastic and osteoclastic process via the Wnt/β-catenin pathway [24]. Osteocytes are the most abundant cells in alveolar bone, but less attention has been paid to the response of bone

cells exposed to mechanical forces and their effects on surrounding cells.

In our study, exosomes derived from osteocytes stimulated by MS altered the PDLSC survival environment. Thus, the mechanical force promoted PDLSC proliferation and differentiation through indirect pathways mediated by exosomes. In addition, we investigated the mechanisms of exosomes in promoting proliferation and osteogenic differentiation. The present study showed that activation of the miR-181b-5p/PTEN/AKT pathway is vital to explain the above phenomena.

Firstly, to further determine the optimal mechanical loading parameters in this experiment, we conducted a preliminary experiment. MLO-Y4 cells were stimulated by cyclic stress of 2%, 4%, 6%, 8%, and 10% shape variables. HPDLSCs were cultured with supernatants from MLO-Y4 cells subjected to different mechanical strengths, and HPDLSCs proliferation was detected by CCK8. The results are shown in(Sup. Fig. 2). The proliferation promoting effect of the 8% group was the highest. Therefore, we considered that 8% shape variable and 0.1 Hz for 30 min could obtain significant experimental effects. Follow-up experiments proved that exosomes derived from osteocytes stimulated by MS improved PDLSC functions.

In order to explore the mechanism of Exosome-MS working, miRNA sequencing was done. Consistent with previously reported [25-28], the results showed that exosome miRNAs are involved in metabolism and cancer processes, endoplasmic reticulum protein processing, focal adhesion protein formation, participating in signaling pathways such as forkhead box O (FoxO) and transforming growth factor-β (TGF-β) (Fig. 4D), which related to cell migration and proliferation. Moreover, miRNAs also involved in a number of growth and apoptosis pathways, affecting cell survival. In addition, miRNAs also involved in cancer, viral and bacteria-related infectious diseases and immune regulation processes. These results showed that miRNAs could participate in the regulation of cell growth and metabolism, and could also participate in the immune system response process caused by bacteria.

These functions are similar to Adipose-derived stem cells (ASCs) that has proven to favor tumor progression in several experimental cancer. ASCs have immune-modulating proprieties mediated by TGF-β1 impairing immune-mediated response to tumor. Moreover, ASCs can induce epithelial to mesenchymal transition in breast cancer cells by acting on multiple pathways, especially through PI3K/AKT signaling.

Recent studies revealed that the Adipocyte-secreted exosomal microRNA (A-SE-MiR) might play important role in tumor progression. They regulated the processes of cell proliferation and apoptosis[29], which were highly similar to the exosomal miRNAs in this study. In present study, miR181b-5p can up-regulate AKT signal by inhibiting PTEN, and promote cell proliferation and inhibited apoptosis, but whether it will cause abnormal proliferation of cells remains to be further explored. However, the results of this study still suggest that proper mechanical stimulation can become a new way to increase the production of therapeutic exosomes.

In addition to the researches in the field of oncology, the proliferation effect of exosomes on periodontal tissues has also been demonstrated in previous studies. MSC exosomes increase PDL cell migration and proliferation through CD73-mediated adenosine receptor activation of pro-survival AKT and ERK signaling. Inhibition of AKT or ERK phosphorylation suppresses PDL cell migration and proliferation [30]. Recent studies have also reported that miRNAs are involved in the development of periodontal disease, especially the process of alveolar bone destruction [31-33]. In addition, mechanically sensitive miRNAs have been found in osteoblasts and have been shown regulate cell differentiation [34]. During bone formation, miRNA molecules are highly enriched in exosomes, and miRNAs play an important role as a "matrix" in bone development through the transfer of exosomes between cells.

In the present study, miR-181b-5p was identified in Exosome-MS (Fig. 5A) and localized in the cytoplasm (Fig. 5B). Previous studies have shown that miR-181 is mainly involved in the progression of cancer [35-37]. In nonsmall cell lung cancer, miR-181 regulated vascular cell adhesion molecule-1(VCAM-1) expression and attenuated tumor cell proliferation and migration[35]. In contrast, there are other reports demonstrating that miR-181 can act as a tumor promoter and contribute to tumor cell malignancy. In acute myeloid leukemia, miR-181 inhibited granulocytic and macrophage-like differentiation of HL-60 cells and CD34+ hematopoietic stem/progenitor cells[38]. It shows that miR181 family has diversity in the regulation of cell behavior. In the present research, luciferase assay and biotin labeling demonstrated

that miR-181b-5p interacts with PTEN (Fig. 5G and 5H). Overexpression of miR-181b-5p inhibited PTEN and activated the AKT pathway and downstream factors (Fig.6). Akt can be activated by small-magnitude mechanical stress [39], and it promotes cell survival by inhibiting apoptosis through inactivating apoptotic proteins [40]. Our results demonstrated that MS upregulates miR-181b-5p in exosomes and activates the AKT pathway by silencing PTEN.

In our experiments, Fig.3 showed that MS promoted HPDLSCs osteogenic differentiation may be related to the upregulation of 181 level in the cytoplasm caused by MS. Other studies have also suggested that miR-181 may be involved in establishing the differentiated phenotype[41]. In addition, MS may also improve the inhibitory effect of inflammation on osteogenic differentiation. Combined Fig. 7, BMP2 and Runx2 expression in PDLSCs was downregulated in the LPS+Exo group, overexpression of miR-181b-5p improved osteogenesis in HPDLSCs under inflammatory conditions, as well as improved BMP2 and Runx2 mRNA expression. MS promoted osteogenic differentiation of HPDLSCs originally, but the ALP and Alizarin Red S staining level, BMP2 and Runx2 expression were down-regulated after transfection with miR181b-5p inhibitor.

It suggested that miR181b-5p not only participated in the cell differentiation process, but also may regulate the immune inflammatory response. Up till now, several studies had provided evidence that miR-181a /b participated in the regulation of inflammatory reactions. For example, a research on pulmonary arterial hypertension (PAH) suggested that miR-181a/b was a protective factor of PAH by targeting endocan to negatively regulate inflammatory states[42]. In experimental model of periapical inflammation induced by TNF-α, miR-181b-5p inhibited the activation of the NF-κB pathway by targeting IL-6, thus inhibited the inflammatory response and promoted the healing of periapical lesion [16].

The results of osteogenic induction experiment prove that the application of Exosome-MS may have a potential role in promoting bone tissue repair. The efficacy of growth factors in bone regeneration surgery has been proven in clinical studies. For example, platelet-rich plasma (PRP) contains multiple growth factors that can induce the migration, proliferation, and differentiation of stem cells[43], which is conducive to the regeneration of soft and hard tissues [44] . The combined application of PRP, ASC and collagen scaffolds can achieve satisfied bone regeneration effect and accelerate wound healing[45]. Unlike the mechanism of growth factors, exosomes internalize into cells, then miRNA silences the target gene mRNA and regulates cell function.

Conclusions

In conclusion, proper mechanical stimulation is beneficial to maintain stem cell properties in an inflammatory environment. The present results not only indicated that the miR-181b-5p/PTEN/AKT signaling pathway functions as a potentially novel mechanism for physiological mechanical force contributing to periodontal homeostasis through the intercellular communication of exosomes in periodontal tissue, but also suggested the potential role of exosomes induced by mechanical force as therapeutic tools for periodontitis and periodontal regeneration.

Declarations

Acknowledgments

Not applicable.

Funding

This study was supported by the 13th 5-Year Comprehensive Investment and First-class Discipline Construction/Stomatology (No. 11601502/xk0126) and Tianjin Medical University Science Fund Project (No. 2016KYZM06).

Availability of data and material

The datasets during and/or analysed during the current study available from the corresponding author on reasonable request.

Author Contributions

M.-j. K. and Y.-L.W. spearheaded and supervised all of the experiments. M.-j.K. and P.-y. L. designed this project. P.-y. L., M.-j. K., P.-f. G., Y.-Y.Y. and F.-f. M. conducted experiments. P.-y.L., P.-f.G., and Z.-h.W. analyzed data. G.-j.T. provided materials. P.-y. L., M.-j.K. and P.-f.G. prepared the manuscript. L.S. provided great help in correcting the grammatical errors and language polishing for this article. All authors reviewed and approved the manuscript.

Ethics approval and consent to participate

Each patient signed an informed consent form for tissue sample donation. This study was approved by the Ethics Committee of Tianjin Medical University Stomatological Hospital (TMUhMEC20190929) and was conducted according to all current ethics guidelines.

Consent for publication

Not applicable.

Competing interests

The authors declare no conflict of interests.

Publisher's Note

Abbreviations

PDL Periodontal ligament

HPDLSC Human periodontal ligment stem cell

ASCs Adipose-derived stem cells

A-SE-MiR Adipocyte-secreted exosomal microRNA

P.g *Porphyromonasgingivalis*

PI3K Phosphatidylinositol-4,5-bisphosphate 3-kinase

Akt Protein kinase B

Runx2 Runt-related transcription factor 2

BMP2 Bone morphogenetic protein-2

PTEN Phosphate and tension homology deleted on chromsome

NTA Nanoparticle Tracking Analysis

FISH Fluorescence in situ hybridization

EdU 5-ethynyl-2’-deoxyuridine

LPS Lipopolysaccharide

TEM Transmission Electron Microscope

miRNA MicroRNA

CCDN1 Cyclin D1

PI3KR1 Phosphoinositide-3-kinase regulatory subunit 1

PI3KCA Phosphatidylinositol-4,5-bisphosphate 3-kinase catalytic subunit alpha

SD Standard Deviation

FoxO forkhead box O

TGF-β transforming growth factor-β

PAH pulmonary arterial hypertension

TNF-α tumor necrosis factor α

VCAM-1 vascular cell adhesion molecule-1

ERK extracellular regulated protein kinases

PRP platelet-rich plasma

References

[1] A. Tomokiyo, N. Wada, H. Maeda, Periodontal Ligament Stem Cells: Regenerative Potency in Periodontium, Stem cells and development, 28 (2019) 974-985.

[2] D.L. Carnes, C.L. Maeder, D.T. Graves, Cells with osteoblastic phenotypes can be explanted from human gingiva and periodontal ligament, J Periodontol, 68 (1997) 701-707.

[3] P. Pavasant, T. Yongchaitrakul, Role of mechanical stress on the function of periodontal ligament cells, Periodontology 2000, 56 (2011) 154-165.

[4] B.M. Seo, M. Miura, S. Gronthos, P.M. Bartold, S. Batouli, J. Brahim, M. Young, P.G. Robey, C.Y. Wang, S. Shi, Investigation of multipotent postnatal stem cells from human periodontal ligament, Lancet (London, England), 364 (2004) 149-155.

[5] J. Liu, Q. Li, S. Liu, J. Gao, W. Qin, Y. Song, Z. Jin, Periodontal Ligament Stem Cells in the Periodontitis Microenvironment Are Sensitive to Static Mechanical Strain, Stem Cells Int, 2017 (2017) 1380851.

[6] X. Song, C.H. Zhu, C. Doan, T. Xie, Germline stem cells anchored by adherens junctions in the Drosophila ovary niches, Science (New York, N.Y.), 296 (2002) 1855-1857.

[7] J. Pizzicannella, A. Gugliandolo, T. Orsini, A. Fontana, A. Ventrella, E. Mazzon, P. Bramanti, F. Diomede, O. Trubiani, Engineered Extracellular Vesicles From Human Periodontal-Ligament Stem Cells Increase VEGF/VEGFR2 Expression During Bone Regeneration, Frontiers in physiology, 10 (2019) 512.

[8] Z. Wang, K. Maruyama, Y. Sakisaka, S. Suzuki, H. Tada, M. Suto, M. Saito, S. Yamada, E. Nemoto, Cyclic Stretch Force Induces Periodontal Ligament Cells to Secrete Exosomes That Suppress IL-1beta Production Through the Inhibition of the NF-kappaB Signaling Pathway in Macrophages, Frontiers in immunology, 10 (2019) 1310.

[9] M. Sato, T. Suzuki, M. Kawano, M. Tamura, Circulating osteocyte-derived exosomes contain miRNAs which are enriched in exosomes from MLO-Y4 cells, Biomed Rep, 6 (2017) 223-231.

[10] F.M. Chen, Y. Jin, Periodontal tissue engineering and regeneration: current approaches and expanding opportunities, Tissue engineering. Part B, Reviews, 16 (2010) 219-255.

[11] S. Ivanovski, C. Vaquette, S. Gronthos, D.W. Hutmacher, P.M. Bartold, Multiphasic scaffolds for periodontal tissue engineering, J Dent Res, 93 (2014) 1212-1221.

[12] C.H. Park, K.H. Kim, Y.M. Lee, Y.J. Seol, Advanced Engineering Strategies for Periodontal Complex Regeneration, Materials (Basel, Switzerland), 9 (2016).

[13] K. Kim, T. Yi, J.H. Yun, Maintained Stemness of Human Periodontal Ligament Stem Cells Isolated After Prolonged Storage of Extracted Teeth, J Periodontol, 87 (2016) e148-158.

[14] Q. Zheng, C. Bao, W. Guo, S. Li, J. Chen, B. Chen, Y. Luo, D. Lyu, Y. Li, G. Shi, L. Liang, J. Gu, X. He, S. Huang, Circular RNA profiling reveals an abundant circHIPK3 that regulates cell growth by sponging multiple miRNAs, Nature communications, 7 (2016) 11215.

[15] B. Liu, Z. Guo, W. Gao, miR-181b-5p promotes proliferation and inhibits apoptosis of hypertrophic scar fibroblasts through regulating the MEK/ERK/p21 pathway, Exp Ther Med, 17 (2019) 1537-1544.

[16] X. Wang, H. Sun, H. Liu, L. Ma, C. Jiang, H. Liao, S. Xu, J. Xiang, Z. Cao, MicroRNA-181b-5p modulates tumor necrosis factor-alpha-induced inflammatory responses by targeting interleukin-6 in cementoblasts, J Cell Physiol, 234 (2019) 22719-22730.

[17] M. Kertesz, N. Iovino, U. Unnerstall, U. Gaul, E. Segal, The role of site accessibility in microRNA target recognition, Nature genetics, 39 (2007) 1278-1284.

[18] M.D. Paraskevopoulou, G. Georgakilas, N. Kostoulas, I.S. Vlachos, T. Vergoulis, M. Reczko, C. Filippidis, T. Dalamagas, A.G. Hatzigeorgiou, DIANA-microT web server v5.0: service integration into miRNA functional analysis workflows, Nucleic Acids Res, 41 (2013) W169-173.

[19] V. Agarwal, G.W. Bell, J.W. Nam, D.P. Bartel, Predicting effective microRNA target sites in mammalian mRNAs, Elife, 4 (2015).

[20] D. Betel, M. Wilson, A. Gabow, D.S. Marks, C. Sander, The microRNA.org resource: targets and expression, Nucleic Acids Res, 36 (2008) D149-153.

[21] V. Stambolic, A. Suzuki, J.L. de la Pompa, G.M. Brothers, C. Mirtsos, T. Sasaki, J. Ruland, J.M. Penninger, D.P. Siderovski, T.W. Mak, Negative regulation of PKB/Akt-dependent cell survival by the tumor suppressor PTEN, Cell, 95 (1998) 29-39.

[22] M. Nakayama, N. Ohara, Molecular mechanisms of Porphyromonas gingivalis-host cell interaction on periodontal diseases, The Japanese dental science review, 53 (2017) 134-140.

[23] L. Imbert, J.C. Auregan, K. Pernelle, T. Hoc, Mechanical and mineral properties of osteogenesis imperfecta human bones at the tissue level, Bone, 65 (2014) 18-24.

[24] L. Zhang, W. Liu, J. Zhao, X. Ma, L. Shen, Y. Zhang, F. Jin, Y. Jin, Mechanical stress regulates osteogenic differentiation and RANKL/OPG ratio in periodontal ligament stem cells by the Wnt/beta-catenin pathway, Biochimica et biophysica acta, 1860 (2016) 2211-2219.

[25] D.P. Bartel, MicroRNAs: genomics, biogenesis, mechanism, and function, Cell, 116 (2004) 281-297.

[26] J. Skog, T. Wurdinger, S. van Rijn, D.H. Meijer, L. Gainche, M. Sena-Esteves, W.T. Curry, Jr., B.S. Carter, A.M. Krichevsky, X.O. Breakefield, Glioblastoma microvesicles transport RNA and proteins that promote tumour growth and provide diagnostic biomarkers, Nat Cell Biol, 10 (2008) 1470-1476.

[27] Y. Zhang, D. Liu, X. Chen, J. Li, L. Li, Z. Bian, F. Sun, J. Lu, Y. Yin, X. Cai, Q. Sun, K. Wang, Y. Ba, Q. Wang, D. Wang, J. Yang, P. Liu, T. Xu, Q. Yan, J. Zhang, K. Zen, C.Y. Zhang, Secreted monocytic miR-150 enhances targeted endothelial cell migration, Molecular cell, 39 (2010) 133-144.

[28] A.G. Ibrahim, K. Cheng, E. Marban, Exosomes as critical agents of cardiac regeneration triggered by cell therapy, Stem cell reports, 2 (2014) 606-619.

[29] P. Gentile, S. Garcovich, Concise Review: Adipose-Derived Stem Cells (ASCs) and Adipocyte-Secreted Exosomal microRNA (A-SE-miR) Modulate Cancer Growth and proMote Wound Repair, Journal of clinical medicine, 8 (2019).

[30] J.R.J. Chew, S.J. Chuah, K.Y.W. Teo, S. Zhang, R.C. Lai, J.H. Fu, L.P. Lim, S.K. Lim, W.S. Toh, Mesenchymal stem cell exosomes enhance periodontal ligament cell functions and promote periodontal regeneration, Acta biomaterialia, 89 (2019) 252-264.

[31] T. Kagiya, S. Nakamura, Expression profiling of microRNAs in RAW264.7 cells treated with a combination of tumor necrosis factor alpha and RANKL during osteoclast differentiation, Journal of periodontal research, 48 (2013) 373-385.

[32] R. Perri, S. Nares, S. Zhang, S.P. Barros, S. Offenbacher, MicroRNA modulation in obesity and periodontitis, J Dent Res, 91 (2012) 33-38.

[33] Y.H. Lee, H.S. Na, S.Y. Jeong, S.H. Jeong, H.R. Park, J. Chung, Comparison of inflammatory microRNA expression in healthy and periodontitis tissues, Biocell : official journal of the Sociedades Latinoamericanas de Microscopia Electronica ... et. al, 35 (2011) 43-49.

[34] Y. Yuan, L. Zhang, X. Tong, M. Zhang, Y. Zhao, J. Guo, L. Lei, X. Chen, J. Tickner, J. Xu, J. Zou, Mechanical Stress Regulates Bone Metabolism Through MicroRNAs, J Cell Physiol, 232 (2017) 1239-1245.

[35] Y. Cao, D. Zhao, P. Li, L. Wang, B. Qiao, X. Qin, L. Li, Y. Wang, MicroRNA-181a-5p Impedes IL-17-Induced Nonsmall Cell Lung Cancer Proliferation and Migration through Targeting VCAM-1, Cellular physiology and biochemistry : international journal of experimental cellular physiology, biochemistry, and pharmacology, 42 (2017) 346-356.

[36] G. Chen, W. Zhu, D. Shi, L. Lv, C. Zhang, P. Liu, W. Hu, MicroRNA-181a sensitizes human malignant glioma U87MG cells to radiation by targeting Bcl-2, Oncology reports, 23 (2010) 997-1003.

[37] S. Schwind, K. Maharry, M.D. Radmacher, K. Mrózek, K.B. Holland, D. Margeson, S.P. Whitman, C. Hickey, H. Becker, K.H. Metzeler, P. Paschka, C.D. Baldus, S. Liu, R. Garzon, B.L. Powell, J.E. Kolitz, A.J. Carroll, M.A. Caligiuri, R.A. Larson, G. Marcucci, C.D. Bloomfield, Prognostic significance of expression of a single microRNA, miR-181a, in cytogenetically normal acute myeloid leukemia: a Cancer and Leukemia Group B study, Journal of clinical oncology : official journal of the American Society of Clinical Oncology, 28 (2010) 5257-5264.

[38] R. Su, H.S. Lin, X.H. Zhang, X.L. Yin, H.M. Ning, B. Liu, P.F. Zhai, J.N. Gong, C. Shen, L. Song, J. Chen, F. Wang, H.L. Zhao, Y.N. Ma, J. Yu, J.W. Zhang, MiR-181 family: regulators of myeloid differentiation and acute myeloid leukemia as well as potential therapeutic targets, Oncogene, 34 (2015) 3226-3239.

[39] Y. Ma, S. Fu, L. Lu, X. Wang, Role of androgen receptor on cyclic mechanical stretch-regulated proliferation of C2C12 myoblasts and its upstream signals: IGF-1-mediated PI3K/Akt and MAPKs pathways, Molecular and cellular endocrinology, 450 (2017) 83-93.

[40] S.R. Datta, H. Dudek, X. Tao, S. Masters, H. Fu, Y. Gotoh, M.E. Greenberg, Akt phosphorylation of BAD couples survival signals to the cell-intrinsic death machinery, Cell, 91 (1997) 231-241.

[41] I. Naguibneva, M. Ameyar-Zazoua, A. Polesskaya, S. Ait-Si-Ali, R. Groisman, M. Souidi, S. Cuvellier, A. Harel-Bellan, The microRNA miR-181 targets the homeobox protein Hox-A11 during mammalian myoblast differentiation, Nat Cell Biol, 8 (2006) 278-284.

[42] H. Zhao, Y. Guo, Y. Sun, N. Zhang, X. Wang, miR-181a/b-5p ameliorates inflammatory response in monocrotaline-induced pulmonary arterial hypertension by targeting endocan, J Cell Physiol, 235 (2020) 4422-4433.

[43] Gentile, Pietro, Bottini, J. Davide, Spallone, Diana, Curcio, B. Cristiano, Cervelli, Valerio, Application of Platelet-Rich Plasma in Maxillofacial Surgery: Clinical Evaluation, Journal of Craniofacial Surgery, 23 (2010) 1580-1582.

[44] V. Cervelli, L. Lucarini, D. Spallone, L. Palla, G.M. Colicchia, P. Gentile, B. De Angelis, Use of Platelet-Rich Plasma and Hyaluronic Acid in the Loss of Substance with Bone Exposure, Advances in Skin & Wound Care, 24 (2011) 176-181.

[45] M.G. Scioli, A. Bielli, P. Gentile, V. Cervelli, A. Orlandi, Combined treatment with platelet-rich plasma and insulin favours chondrogenic and osteogenic differentiation of human adipose-derived stem cells in three-dimensional collagen scaffolds, Journal of Tissue Engineering & Regenerative Medicine, (2016).

Supplemental Figures

Sup.Fig. 1. Characterization of HPDLSCs.

(A) Morphology of HPDLSCs under an inverted microscope (scale bar=50μm).

(B) CFU-F assay result (scale bar:1mm). (C) Alizarin Red staining after osteogenic induction (scale bar: 200 μm). (D) Oil red O staining after adipogenic induction (scale bar: 100 μm). (E) Flow cytometry analyses of the positive surface biomarkers CD73, CD90 and CD146, negative biomarker CD45.

Sup. Fig. 2 The effects of supernatants from MLO-Y4 cells stimulated by different mechanical forces on HPDLSC proliferation (*P < 0.05 and **P < 0.01).

Sup. Fig. 3 Upregulated miRNA levels in Exosome and Exosome-MS were analyzed using real time-PCR. (*P < 0.05 and **P < 0.01)

Figures

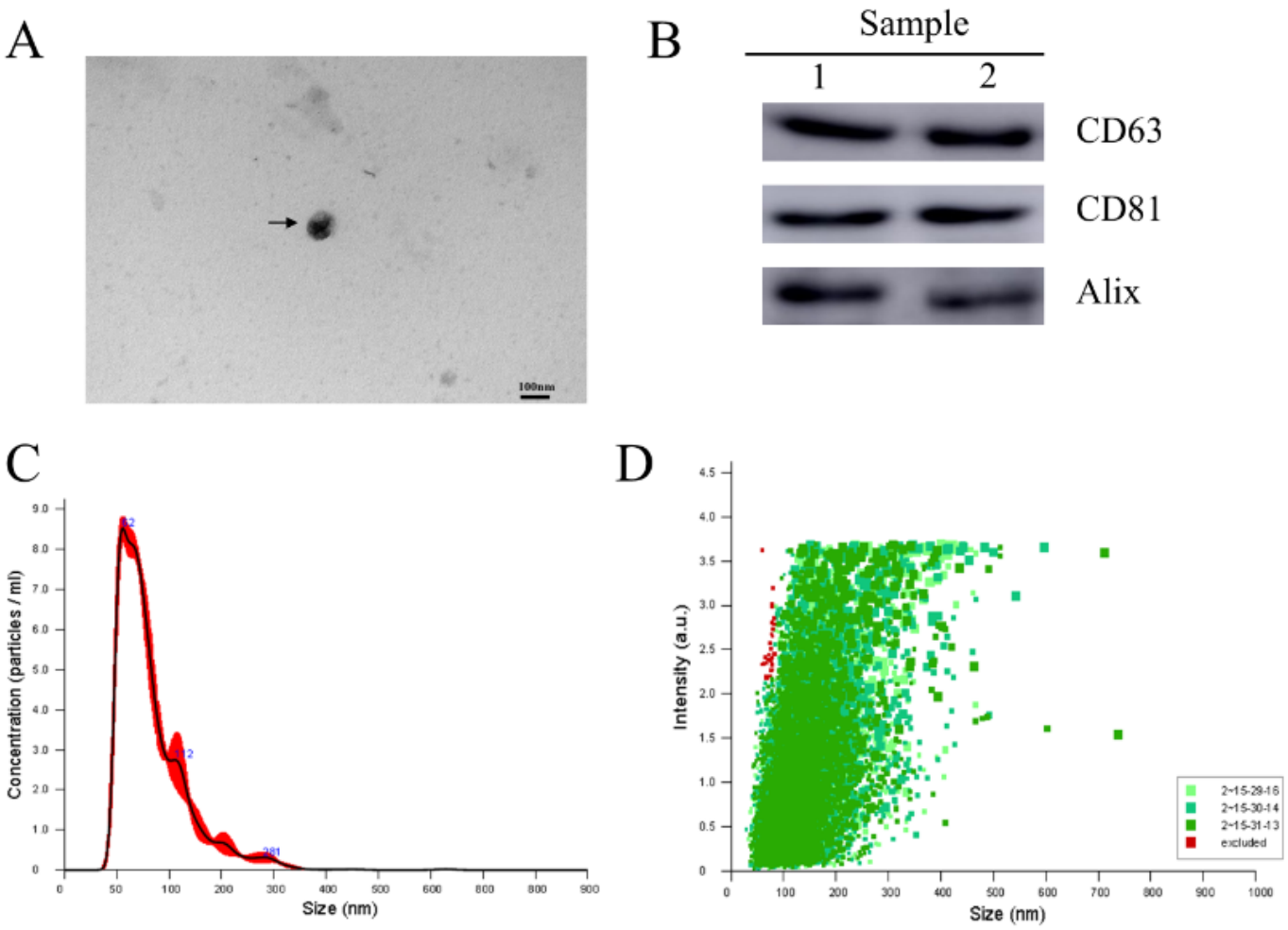

Figure 1

Characterization of exosomes derived from MLO-Y4 culture supernatants. (A) Morphology of MLO-Y4-Exosomes identified by TEM, bar=100nm. (B) Western blotting assay of the surface biomarkers CD63, CD81 and Alix. (C) Particle size and concentration of MLO-Y4-Exos measured by NTA. (D) Particle size distribution intensity.

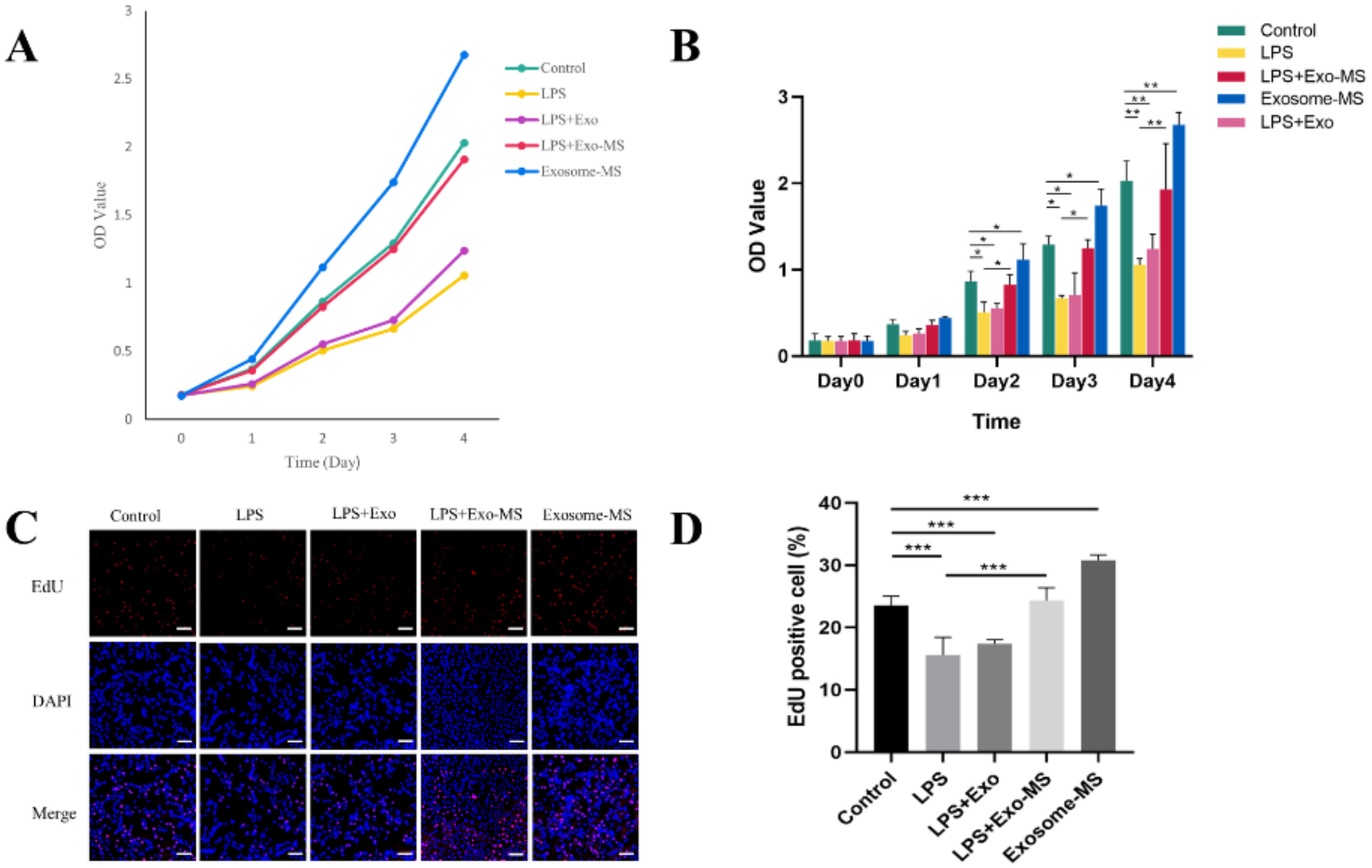

Figure 2

Effects of Exosome-MS on proliferation of HPDLSCs. The cell proliferation ability of HPDLSCs treated with Exosome or Exosome-MS together with or without Pg.LPS. (A) The cell proliferation curve of HPDLSCs from day 0 to day 4. (B) The OD values are shown for each group. EdU staining was used to reflect DNA replication activity of HPDLSCs, as observed by (C) Confocal fluorescence microscopy images (scale bar:100 μm).. (D) EdU-positive percentage was calculated by ImageJ in different treatment groups (*P < 0.05, **P < 0.01, and ***P < 0.001).

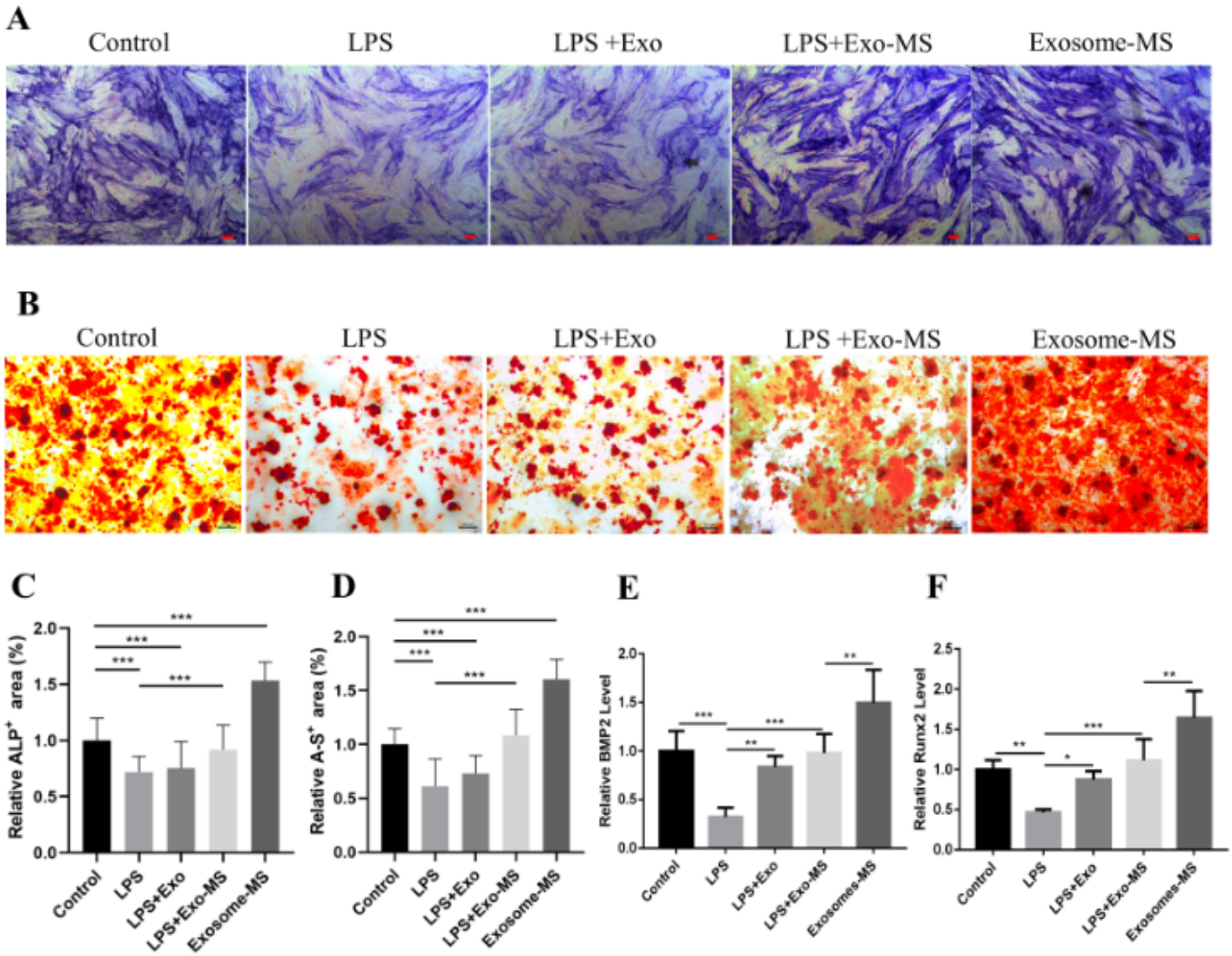

Figure 3

Effects of Exosome-MS on osteogenic differentiation of HPDLSCs. ALP and Alizarin red staining were used to evaluate the osteogenic differentiation of HPDLSCs in different treatment groups. (A) ALP staining (scale bar:100 μm). (B) Alizarin red staining (scale bar:200 μm). (C) Relative ALP-positive area as calculated by ImageJ. (D) Relative Alizarin red-positive area as calculated by ImageJ. (E and F) The expression levels of BMP2 and Runx2 in different groups were verified using real time-PCR (*P < 0.05, **P < 0.01, and ***P < 0.001).

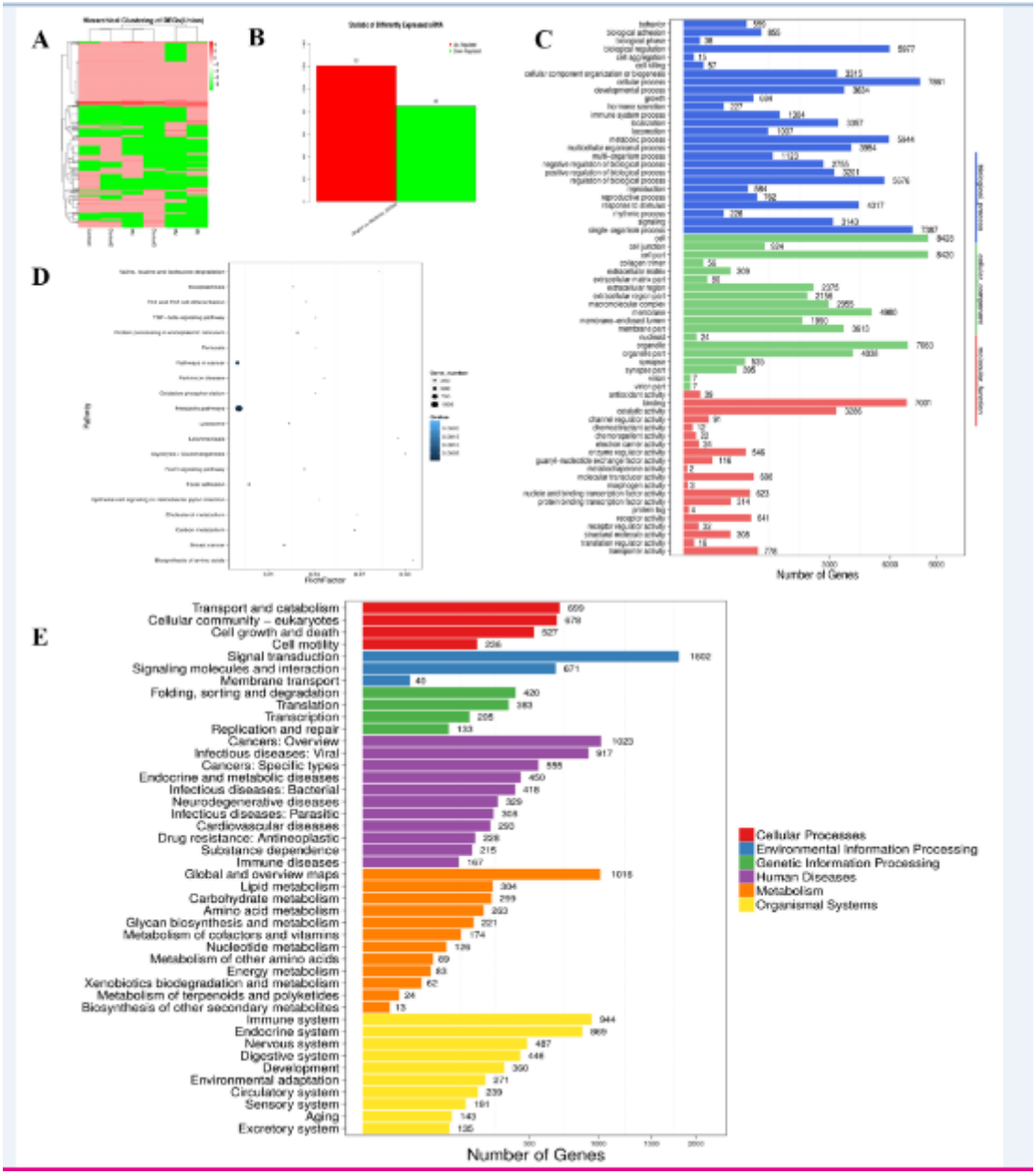

Figure 4

Analysis of functional attributes connected to Exosome-MS changes in gene sets and signaling pathways. miRNA-seq comparison between the Exosome and Exosome-MS groups. (A) Heat map showing differentially expressed miRNAs. (B) Upregulated and downregulated miRNAs. (C) GO biological process classification of the genes. (D) Significantly enriched gene ontology terms are shown in the plot. (E) KEGG functional enrichment analysis.

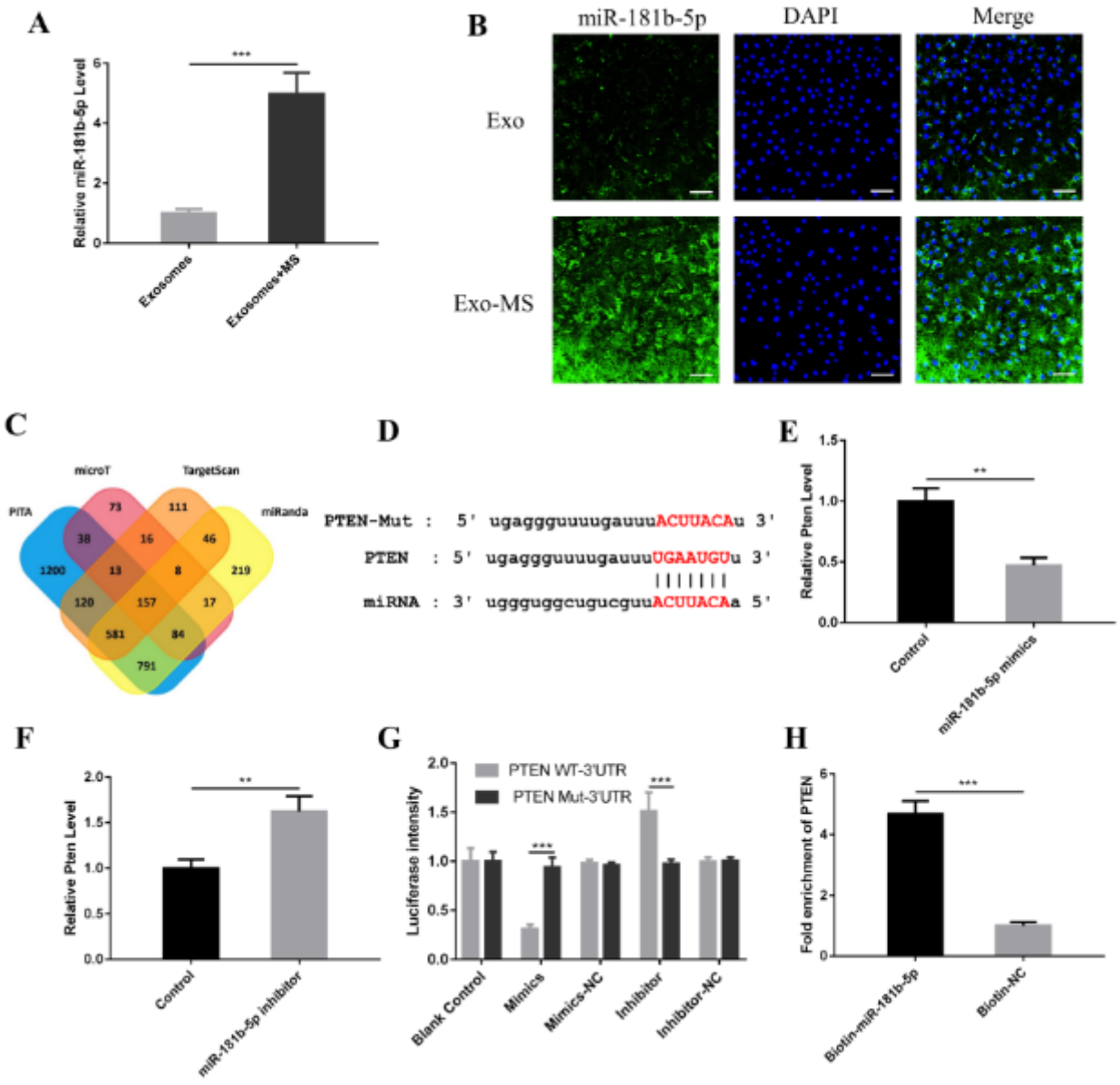

Figure 5

PTEN is a target gene of miR-181b-5p. (A) The levels of miR-181b-5p in Exosome and Exosome-MS were detected using real time-PCR. (B) Cell localization of miR-181b-5p in HPDLSCs treated with exosomes according to FISH (scale bar:100 μm).. (C) The number of target genes of miR-181b-5p predicted by the PITA, microT, TargetScan and miRnada databases. In total, 157 crossover genes were obtained. (D) The binding site between miR-181b-5p and PTEN. (E) real time-PCR showed PTEN level when HPDLSCs were transfected with miR-181b-5p mimics. (F) real time-PCR showed PTEN level when HPDLSCs were transfected with miR-181b-5p inhibitor. (G) Fluorescence intensity was calculated by ImageJ. (H) Enrichment information for biotin-labeled miR-181b-5p binding to PTEN (*P < 0.05, **P < 0.01, and ***P < 0.001).

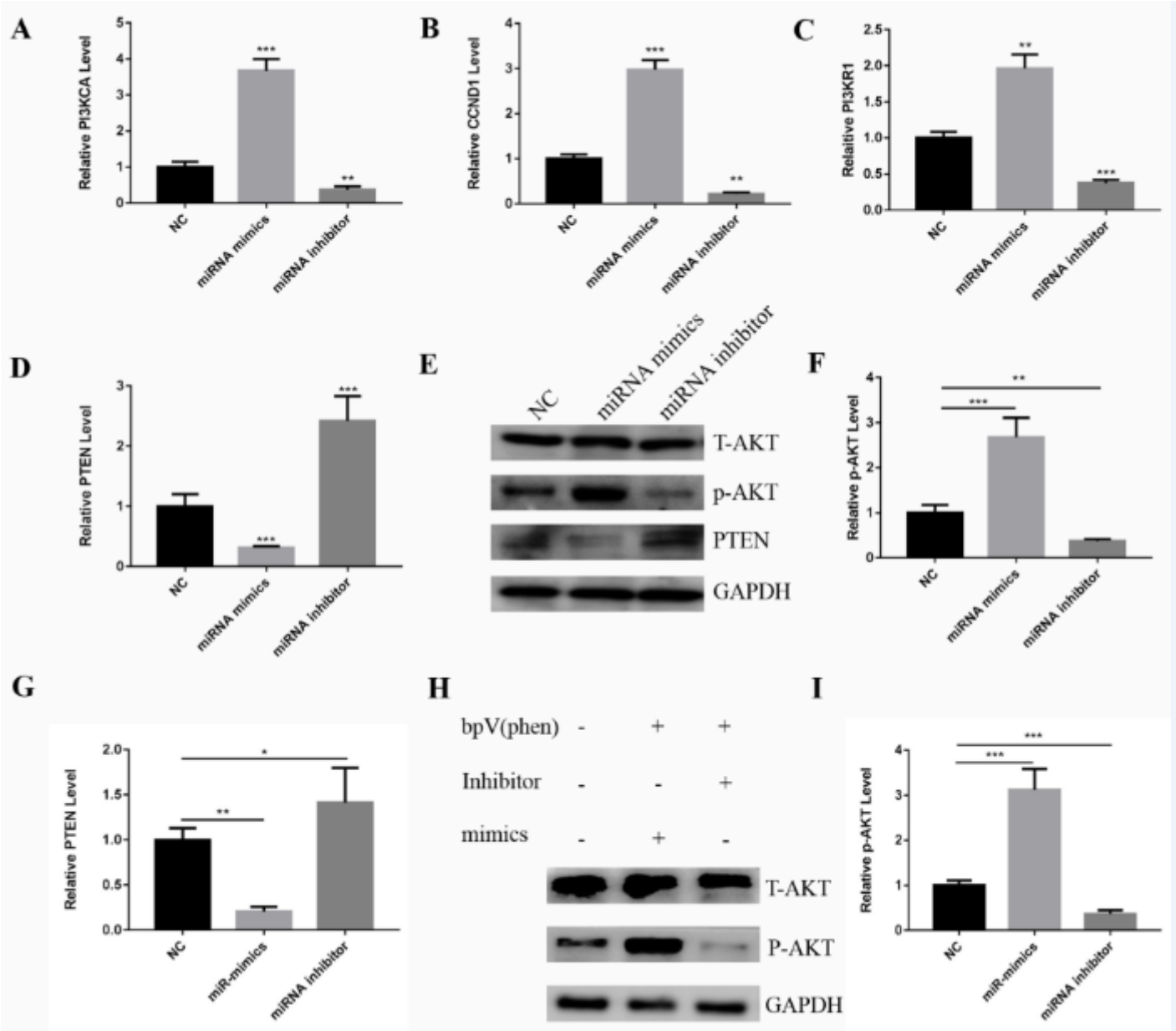

Figure 6

Exosomal miR-181b-5p regulates HPDLSC proliferation through the PTEN/AKT signaling pathway. (A-D) The expression levels of genes in the PTEN/AKT signaling pathway including CCND1, PIK3CA, PIK3R1 and PTEN after inhibition or overexpression of miR-181b-5p were verified using real time-PCR. (E) Western blotting assay was performed to evaluate the expression of PTEN and p-AKT. (F and G) Quantitative analysis of western blotting assay using ImageJ. (H) Western blotting assay showed the effect of PTEN inhibitor and miR-181b-5p on expression of pAKT. (I) Quantitative analysis of western blotting assay using ImageJ (*P < 0.05, **P < 0.01, and ***P < 0.001).

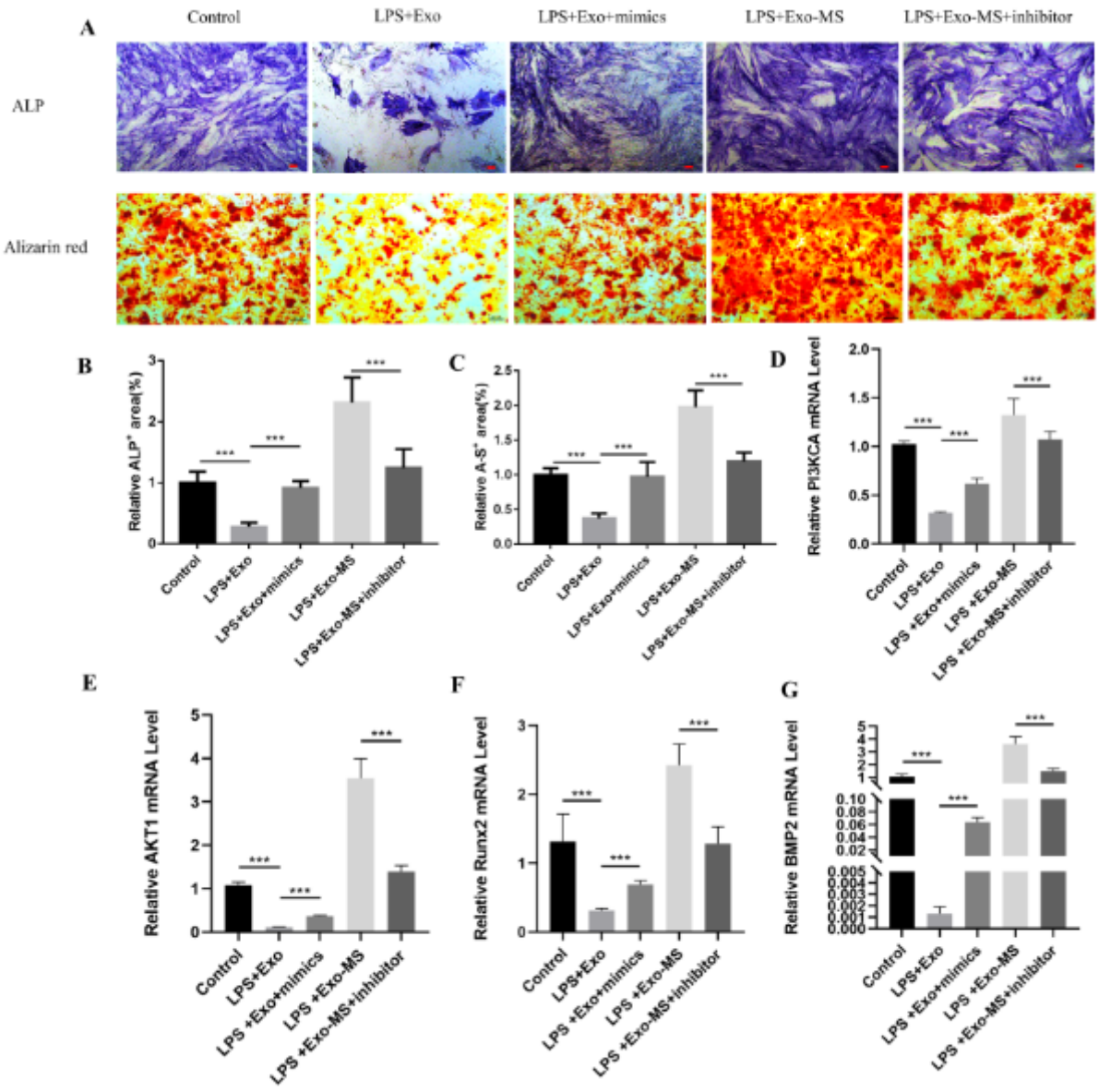

Figure 7

Exosome-MS regulates HPDLSC osteogenic differentiation by miR-181b-5p. Inhibiting or overexpressing miR-181b-5p changes the osteoblast differentiation ability of HPDLSCs with LPS stimulation between the Exosome and Exosome-MS group. (A) ALP staining (scale bar: 100 μm) and Alizarin red staining (scale bar:200 μm). (B and C) Quantitative analysis of staining using ImageJ. (D-G) The expression of genes including PIK3CA, AKT1, Runx2 and BMP2.

Supplementary Files

This is a list of supplementary files associated with this preprint. Click to download.

- Sup.Fig.2.tif
- Sup.Fig.1.tif

- Sup.Fig.3.tif